Neutron-diffraction studies and bond valence sums of charge neutrally doped $Nd_{1-2x}Ca_xTh_xBa_2Cu_3O_{7-\delta}$

P. Lundqvist and Ö. Rapp
Solid State Physics, The Royal Institute of Technology, S-100 44 Stockholm, Sweden

R. Tellgren
Inorganic Chemistry, Ångström Laboratory, Uppsala University, Box 538, S-751 21 Uppsala, Sweden

I. Bryntse
Inorganic Chemistry, Arrhenius Laboratory, Stockholm University, S-106 91 Stockholm, Sweden
(Received 19 February 1997)

Equal amounts of Ca and Th have been doped into the $Nd_{1-2x}Ca_xTh_xBa_2Cu_3O_{7-\delta}$ superconductor with $x=0$, 0.015, 0.03, 0.05, and 0.10. This causes a fast and linear decrease of the superconducting transition temperature, T_c. A single orthorhombic phase was observed with x-ray diffraction except for weak additional lines for the $x=0.10$ sample, suggesting a solubility limit below $x=0.10$. Neutron-diffraction measurements were performed and bond valence sums (BVS's) were calculated. The results showed a small increase in the Cu2-O4 distance and a nearly constant Cu2 valence. The total hole density in the plane, V_- as defined by Tallon, remains almost constant with doping in contrast to the decrease observed for Ca-Pr doping. Other results from the BVS calculations also indicate differences between Ca-Th and Ca-Pr doping in the $NdBa_2Cu_3O_{7-\delta}$ compound. [S0163-1829(97)01829-8]

I. INTRODUCTION

Four-valent Th does not easily enter into the rare-earth position of the RE-123 superconductors. However, when co-substituting Th with an equal amount of two-valent Ca, it was found that orthorhombic $Y_{1-2x}Ca_xTh_xBa_2Cu_3O_{7-\delta}$ could be obtained up to a solubility limit of about $x=0.10$.[1] The changes of the lattice parameters and of the oxygen occupation were negligible,[2] thus suggesting a conserved hole concentration. Since Ca and Th are not expected to be magnetic and the distortion of the lattice is minimal, the strong linear decrease of the critical temperature, T_c of[3] $-dT_c/dx=180$ K is surprising. This suppression of T_c is even larger than in similarly charge neutrally Ca-Pr doped Y-123, where $-dT_c/dx=97$ K.[4] The linear decrease of T_c in this case has been assumed to arise from magnetic pair breaking or hole localization.[4,5] Another suggestion involves interatomic distances and corresponding charge transfers as inferred in Ca-Pr doped Nd-123 from neutron-diffraction experiments and bond valence sum (BVS) calculations.[6] It has also been found that the linear depression rate of T_c in Ca-Pr doped 123 increases with the ionic radius of the host,[7] and in Nd-123 the large value of $-dT_c/dx=206$ K was observed.[6]

In the present paper we have further studied the interesting behavior of Ca-Th doping. Nd-123 was chosen as the host, with the expectation to obtain as large effect as possible on T_c, and significant structural changes. Earlier studies of Ca-Th doped Y-123 sometimes showed scattered trends in structural changes. In the present study of five samples of Nd-123 doped with Ca-Th, we could use an improved experimental setup with more detectors and a more intense neutron beam. We present results for these samples from electrical resistance properties, structural studies by x-ray and neutron diffraction, and calculations of bond valence sums. Comparisons will be made with corresponding results for Ca-Pr doped samples.

II. EXPERIMENTAL DETAILS

A. Sample preparation and characterisation techniques

Samples of $Nd_{1-2x}Ca_xTh_xBa_2Cu_3O_{7-\delta}$ with $x=0$, 0.015, 0.03, 0.050, and 0.10 were prepared by standard solid-state methods. Starting materials were regent grade Nd_2O_3, $BaCO_3$, CuO, ThO_2, and $CaCO_3$. The samples were pressed into pellets and calcined three times at 900, 920, and 920 °C, respectively, with intermediate grindings. They were then annealed in flowing oxygen at 460 °C for 3 days and the temperature was then decreased to room temperature at a rate of 12 °C per h.

The x-ray powder diffraction patterns were recorded in a Guinier-Hägg focusing camera using Cu $K\alpha$ radiation with Si as an internal standard.[8] The electrical resistivity was measured with a standard four-probe dc method. Leads were attached by silver paint and heat treated at 300 °C in flowing oxygen for half an hour. T_c was taken as the midpoint of the resistive transition.

B. Neutron diffraction

The neutron powder diffraction data were recorded at room temperature at the Swedish research reactor R2 in Studsvik. A double-monochromator system using the (220) planes of two copper crystals gave a wavelength of 1.470 Å and a neutron flux at the sample position of approximately 2×10^6 cm^{-2} s^{-1}. The powdered samples were contained in vanadium tubes with only 6 mm diameter due to the large absorption of neutrons in Nd. Data were collected with 35

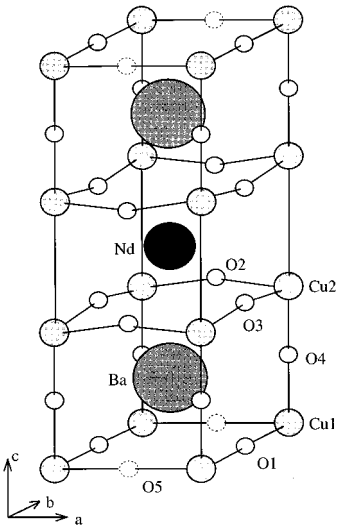

FIG. 1. Notation of atoms of $NdBa_2Cu_3O_{7-\delta}$.

^{3}He detectors which were scanned in steps of 0.05° covering the range 4.00°–139.95° in 2θ. Structure refinements were performed with the Rietveld method[9] using the FULLPROF program[10] and the orthorhombic space group *Pmmm*. Anisotropic displacement parameters at the Cu-O chain sites led to better refinements. The displacement parameters at the oxygen vacant, O5, site were set to the same values as those at the O1 site except for a switch between the basal plane axial x and y directions. At all other sites isotropic displacement parameters were used. Most atomic positions were considered to be fully occupied, with three exceptions: (1) the Nd site where the occupation factors were refined with the condition that the doping ratios were correct, (2) the chain oxygen O1, and (3) O5 positions to register any oxygen disorder and to determine the oxygen concentration. A unit cell is shown in Fig. 1 for easy reference to structural notations. A neutron-diffraction pattern for $Nd_{0.9}Ca_{0.05}Th_{0.05}Ba_2Cu_3O_{7-\delta}$ is shown in Fig. 2 as an example.

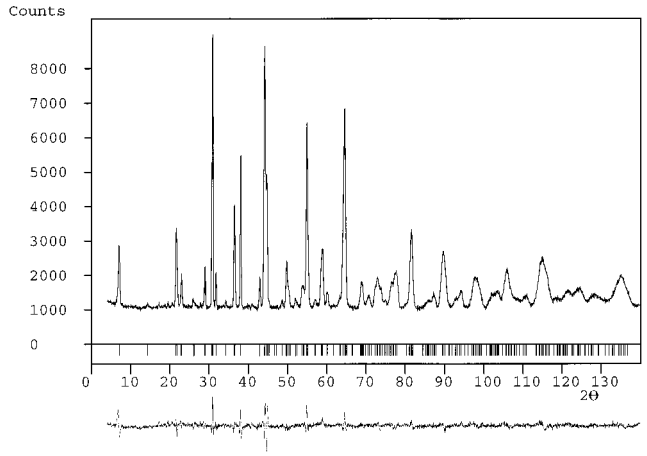

FIG. 2. Neutron-diffraction results for $Nd_{0.90}Ca_{0.05}Th_{0.05}Ba_2Cu_3O_{7-\delta}$. In the panel below the data the positions of the indexed lines are shown. The difference between calculated and observed intensities are shown below the main panel (with the same ordinate scale as in the main panel).

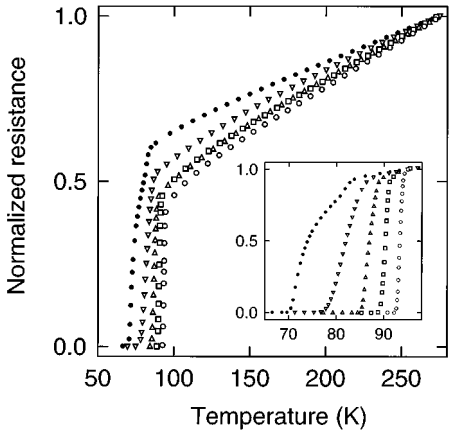

FIG. 3. Electrical resistance of $Nd_{1-2x}Ca_xTh_xBa_2Cu_3O_{7-\delta}$. Data have been normalized to $T=275$ K. The inset shows the superconducting transitions normalized to the resistance at 95 K. Curves from right to left are for $x=0$, 0.015, 0.030, 0.05, and 0.10 respectively. The transition for $x=0.10$ suggests that the solubility limit has already been reached.

C. Bond valence sum calculations

The method used for bond valence sum (BVS) calculations was similar to that described in some detail previously.[6] Therefore, only a few details are mentioned below. The atomic valence of an atom is assumed to be distributed between the bonds that it forms. BVS for atom i is then $V_i=\Sigma s_j=\Sigma\ \exp[(R_0-R_{ij})/0.37]$ where s_j is the valence of one bond, and the sum is over all neighbors j. The constant 0.37 was empirically determined.[11] R_0 represents the length of a bond of unit valence,[11] and R_{ij} is the experimentally determined distance between atoms i and j. R_0 was taken to be 1.600, 1.679, and 1.730 Å for Cu^{1+}, Cu^{2+}, and Cu^{3+}, respectively.[12,13] R_0 for the other atoms were taken from Brown and Altermatt,[11] except for Pr^{4+} and Th^{4+}, for which R_0 was calculated to be 2.154 and 2.070 Å, respectively, with the same method as in Ref. 11. The copper BVS was calculated using the formulas suggested by Tallon,[12] and the BVS for Pr as described in Ref. 6.

BVS for oxygen was obtained by taking into account the valence of Cu and Pr.[6] The hole density in the plane ($V_-=2+V_{Cu2}-V_{O2}-V_{O3}$) and the preference for distribution of holes at oxygen sites ($V_+=6-V_{Cu2}-V_{O2}-V_{O3}$) as suggested by Tallon[12] were also calculated.

III. RESULTS AND DISCUSSION

A. Electrical resistivity

The normalized electrical resistivity vs temperature, shown in Fig. 3, was found to be linear for all doping levels. The superconducting transition widths, from 90 to 10 % of the resistance drop, were 1.1, 1.4, 2.6, 6.2, and 9.8 K for $x=0$, 0.015, 0.03, 0.05, and 0.10, respectively. For the sample with $x=0.10$ a double transition was observed suggesting a solubility limit below $x=0.10$. Increased doping concentration resulted in a strong increase of the resistivity and a decrease in the temperature coefficient of resistance, as shown in Fig. 4, which suggests a weakening of the metallic state with increasing Ca-Th concentration. In both cases the

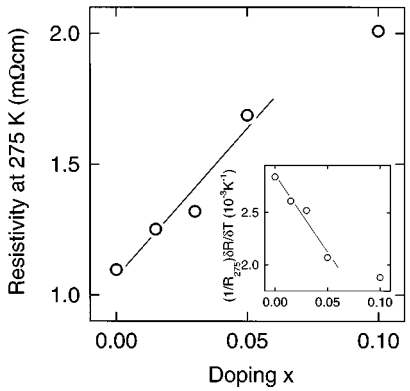

FIG. 4. The electrical resistivity at 275 K vs doping concentration. Inset: The temperature coefficient of resistance at 275 K. The lines are guides to the eye and were fitted to the data up to $x = 0.05$.

10% sample showed small deviations from the trends of the samples with less doping, again pointing to a solubility limit slightly below $x = 0.10$.

T_c vs concentration is shown in Fig. 5. A linear relation between T_c and doping is well obeyed in the orthorhombic phase, and the depression rate is $-dT_c/dx = 232$ K. This is apparently the strongest suppression rate observed in charge neutrally doped 123 compounds.

B. X-ray diffraction

X-ray powder diffraction was used mainly as a convenient way to characterize the samples and to ascertain a single orthorhombic phase in the sensitive technique used. All samples showed reflections from orthorhombic 123 and they were single phase at our low doping levels with the exception of the $x = 0.10$ sample. The latter showed very weak impurity reflections supporting a solubility limit slightly below $x = 0.10$. Th was earlier found not to substitute Y in 123 compounds unless codoped with Ca, and the solubility limit in this case was also around 10%.[1]

C. Neutron-diffraction results

Results from Rietveld refinements of diffraction data are given for all samples in Table I. Compared to earlier measurements,[2,6] the improvements of the experimental technique have led to a higher neutron count even with reduced measuring time, to smaller background at low θ values, and to quite small R values of the refinements, particularly considering the high absorption of neutrons by Nd atoms. These results therefore indicate a good quality of the data.

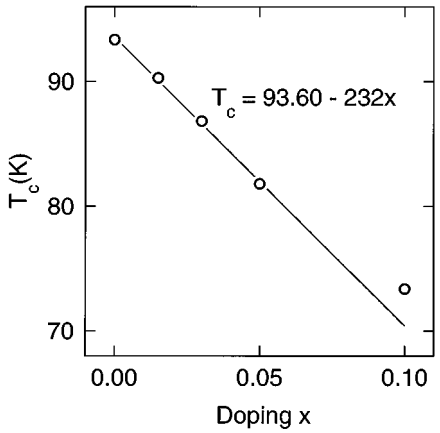

FIG. 5. T_c vs x for $Nd_{1-2x}Ca_xTh_xBa_2Cu_3O_{7-\delta}$. The straight line shown was fitted to the data up to $x = 0.05$.

The results for the pure Nd sample agree with earlier results.[6,14] Structural changes with Ca-Th doping are rather small, and in general smaller than for $Y_{1-2x}Ca_xTh_xBa_2Cu_3O_{7-\delta}$.[2] An exception is the large decrease of the c-axis length with doping in Nd-123, shown in Fig. 6, in contrast to the rather constant c-axis length in Y-123.[2] This is not surprising since the radius of Nd is almost as large as that of Ca, while Th is about 5% smaller and Y about 10% smaller than Ca.[15] Together with a small decrease of the b axis this gives a decreasing cell volume. The increase of the a axis and the decrease of the b-axis cause the orthorhombicity to decrease slightly as can be seen in the inset of Fig. 6. This is accompanied by a small increase in the O5 occupancy, pointing to an increased disorder in the Cu-O chains with increasing Ca-Th content as has also been seen in the $Y_{1-2x}Ca_xTh_xBa_2Cu_3O_{7-\delta}$.[2] The total oxygen occupation is constant within the measurement accuracy, indicating, as does the small changes in structure, that the hole concentration is fairly constant.

The sensitivity of superconducting properties to small changes in the Cu1-O4 distance has been noticed by several authors and considered to be important for the charge transfer from the Cu-O chains to the planes. As can be seen in the top panel of Fig. 7 the Cu1-O4 distance stays fairly constant with doping. The small increase in this distance inferred previously[2] for Ca-Th doping in Y-123 is within the present experimental uncertainty. For $Y_{1-2x}Ca_xPr_xBa_2Cu_3O_{7-\delta}$ the Cu1-O4 distance increased slightly with x,[16] and in the case of $Nd_{1-2x}Ca_xPr_xBa_2Cu_3O_{7-\delta}$ the dominating trend was a decrease with x of the Cu1-O4 distance.[6] Variations in the Cu1-O4 distance are thus apparently unrelated to the large effect on T_c in $Nd_{1-2x}Ca_xTh_xBa_2Cu_3O_{7-\delta}$.

The Cu2-O4 distance, on the other hand, increases with doping with the exception of the 10% sample above the solubility limit. The present results are compared in the bottom panel of Fig. 7 with Ca-Th doping in Y-123 and Ca-Pr doping in Nd- and Y-123. The concentration dependence of the Cu2-O4 distance is similar in Ca-Th and Ca-Pr doped Nd-123. This conclusion is apparently valid also for the same dopings in Y-123, as illustrated in the upper part of the bottom panel in Fig. 7. From these observations it could be tempting to suggest that the Cu2-O4 bond length is related to the depression of T_c.

D. Bond valence sums

In order to estimate the effect of varying bond distances on the valences of the different atoms it is useful to calculate bond valence sums (BVS's). Although this method is empirical, it can nevertheless help to identify important trends when a series of related and similarly prepared samples are compared.

The result for the BVS is shown in Table II for the present $Nd_{1-2x}Ca_xTh_xBa_2Cu_3O_{7-\delta}$ samples. In Table III a similar calculation is given for $Y_{1-2x}Ca_xTh_xBa_2Cu_3O_{7-\delta}$ with dif-

TABLE I. Structural parameters for $Nd_{1-2x}Ca_xTh_xBa_2Cu_3O_{7-\delta}$. The relative position along the c-axis, z, occupation numbers, n, isotropic displacement parameters, B, and oxygen contents, δ, are given. The occupation numbers of Ca and Th were set to be the same in the analysis. For the O(1) atom anisotropic displacement parameters were used of the form $\exp-(\beta_{11}h^2+\beta_{22}k^2+\beta_{33}l^2)$. Numbers in parentheses are statistical standard deviations of the least significant digit/s.

x (%)		0	1.5	3.0	5.0	10.0
a (Å)		3.8623(2)	3.8636(2)	3.8666(2)	3.8684(2)	3.8679(2)
b (Å)		3.9122(2)	3.9113(3)	3.9115(3)	3.9101(3)	3.9098(3)
c (Å)		11.748(1)	11.741(1)	11.736(1)	11.730(1)	11.732(1)
V (Å^3)		177.52(3)	177.43(3)	177.49(4)	177.43(4)	177.41(4)
Nd	B (Å^2)	0.17(7)	0.17(8)	0.15(8)	0.33(9)	0.37(9)
	n	0.994(8)	0.962(4)	0.930(4)	0.901(4)	0.800(4)
Ca	n		0.014(4)	0.030(4)	0.050(4)	0.100(4)
Th	n		0.014(4)	0.030(4)	0.050(4)	0.100(4)
Ba	z	0.1815(3)	0.1817(4)	0.1816(4)	0.1817(4)	0.1820(4)
	B (Å^2)	0.50(6)	0.51(8)	0.45(8)	0.46(8)	0.44(8)
Cu(1)	B (Å^2)	0.65(7)	0.70(8)	0.87(8)	0.89(9)	0.88(9)
Cu(2)	z	0.3490(2)	0.3492(2)	0.3496(2)	0.3498(2)	0.3499(2)
	B (Å^2)	0.47(4)	0.46(5)	0.55(5)	0.46(5)	0.53(5)
O(2)	z	0.3706(3)	0.3701(4)	0.3707(5)	0.3705(5)	0.3701(5)
	B (Å^2)	0.66(8)	0.76(9)	0.83(10)	0.80(10)	0.72(11)
O(3)	z	0.3709(4)	0.3715(4)	0.3709(5)	0.3715(5)	0.3708(5)
	B (Å^2)	0.67(7)	0.59(8)	0.70(9)	0.61(9)	0.54(10)
O(4)	z	0.1577(3)	0.1576(3)	0.1579(4)	0.1575(4)	0.1580(4)
	B (Å^2)	0.74(8)	0.84(9)	0.96(9)	1.02(10)	1.00(10)
O(1)	β_{11} (Å^2)	0.069(7)	0.083(9)	0.097(10)	0.097(10)	0.103(11)
	β_{22} (Å^2)	0.001(4)	−0.000(5)	0.005(5)	0.001(5)	0.009(6)
	β_{33} (Å^2)	0.0026(3)	0.0022(4)	0.0020(4)	0.0023(4)	0.0029(4)
	n	0.96(2)	0.95(2)	0.92(2)	0.92(2)	0.92(2)
O(5)	n	0.07(2)	0.07(2)	0.11(2)	0.12(2)	0.12(2)
δ		−0.02(3)	−0.02(3)	−0.03(3)	−0.04(3)	−0.04(4)
R_p (%)		3.39	3.48	3.24	3.35	4.32
R_{wp} (%)		4.64	4.65	4.37	4.62	6.07
R_{expt} (%)		2.84	2.60	2.49	2.60	2.94
R_{Bragg} (%)		3.53	4.27	4.60	4.47	4.52

fraction data from Ref. 2, to reach more firm conclusions on common and different trends when Ca-Th and Ca-Pr doping is compared.

It can first be noted that Cu2 has a near constant valence for Ca-Th doping in both Y and Nd hosts. The observation was also made for Ca-Pr doping in the same hosts,[6] and supports that charge neutral dopings are indeed obtained. The results are compared in Fig. 8, with Y-123 doped with Pr only, as calculated with the same methods as presently used,[6] and with structural data from Neumeier *et al.*[17] In that case the Cu2 valence decreases with doping as expected for a Pr valence >3.

The preference for holes to go to the oxygen atoms in the CuO_2 plane, V_+, was linearly correlated by Tallon to the maximum attainable T_c in a particular alloy system.[12] He found an increase in T_c with an increase in V_+. With charge neutral dopings we expect the parabolic term in the relation between T_c and doping concentration to be reduced to a constant. In our case therefore, for each Ca concentration, T_c of the co-doped sample is close to the maximum T_c for that doping. However, the results in Tables II and III show a

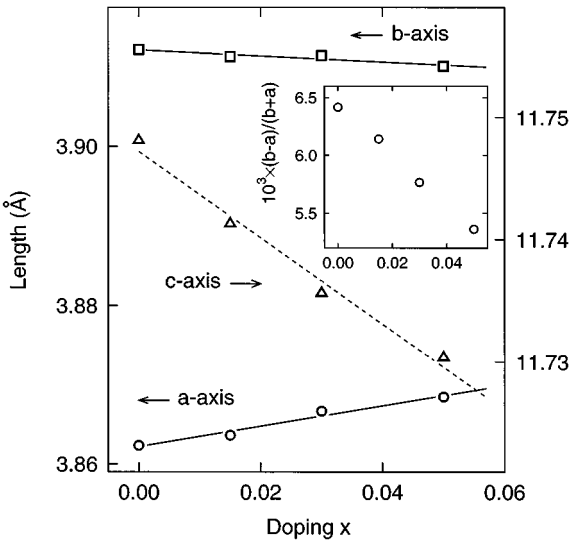

FIG. 6. Cell parameters of $Nd_{1-2x}Ca_xTh_xBa_2Cu_3O_{7-\delta}$ from neutron-diffraction data. The inset shows the orthorhombicity vs doping.

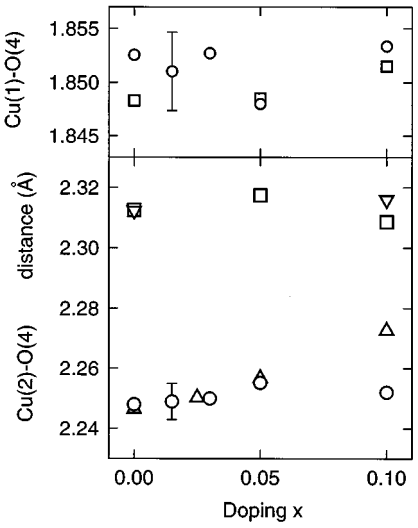

FIG. 7. Top panel: Cu1-O4 distance for ○ $Nd_{1-2x}Ca_xTh_xBa_2Cu_3O_{7-\delta}$ (present data) and □, $Y_{1-2x}Ca_xTh_xBa_2Cu_3O_{7-\delta}$ (data from Ref. 2). Bottom panel: Cu2-O4 distance for CaTh doping as above: △, $Nd_{1-2x}Ca_xPr_xBa_2Cu_3O_{7-\delta}$ (data from Ref. 6); and ▽, $Y_{1-2x}Ca_xPr_xBa_2Cu_3O_{7-\delta}$ (data from Ref. 16). Estimated error bars are shown for two samples. $x=0.1$ is at or slightly above the solubility limit for the Ca–Th doped samples.

decrease in T_c with an increase in V_+. The relative change in V_+ vs T_c is of similar magnitude as for Ca-Pr doping,[6] but the sign is opposite for Ca-Th doping.

Another interesting result is that the total hole density in the planes, V_-, stays almost constant with Ca-Th doping, or possibly increases somewhat. T_c vs V_- is compared in Fig. 9 with two charge doped systems; doping with Pr only in Y-123 and oxygen depletion, where V_- as expected decreases strongly with addition of Pr or removal of oxygen.

TABLE II. Bond valence sums BVS's for $Nd_{1-2x}Ca_xTh_xBa_2Cu_3O_{7-\delta}$. V_- and V_+ give the average hole density in the plane and preference for distribution of holes on oxygen sites, respectively, as defined by Tallon (Ref. 12). The $\overline{\text{Nd}}$ is an average valence on the rare-earth position taking into account the Ca and Th valences and occupation.

x (%)	0	1.5	3.0	5.0	10.0
Nd	3.014	3.021	3.018	3.033	3.001
$\overline{\text{Nd}}$	3.014	3.003	2.982	2.972	2.881
Ba	2.169	2.170	2.171	2.170	2.184
Cu(1)	2.335	2.347	2.350	2.391	2.366
Cu(2)	2.124	2.124	2.122	2.116	2.129
O(1)	1.801	1.801	1.802	1.808	1.800
O(2)	2.039	2.037	2.032	2.027	2.016
O(3)	2.031	2.031	2.023	2.019	2.005
O(4)	1.974	1.977	1.971	1.978	1.970
O(5)	1.834	1.833	1.832	1.836	1.828
V_-	0.055	0.056	0.067	0.070	0.107
V_+	−0.194	−0.192	−0.177	−0.162	−0.150
T_c (K)	93.35	90.29	86.83	81.80	73.37

TABLE III. Bond valence sums (BVS's) for $Y_{1-2x}Ca_xTh_xBa_2Cu_3O_{7-\delta}$. Calculations were based on data from Ref. 2.

x (%)	0	5.0	10.0
Y	2.887	2.820	2.820
$\overline{\text{Y}}$	2.887	2.823	2.824
Ba	2.170	2.145	2.166
Cu(1)	2.347	2.253	2.321
Cu(2)	2.186	2.175	2.181
O(1)	1.830	1.779	1.809
O(2)	2.040	2.036	2.029
O(3)	2.018	2.015	2.008
O(4)	2.009	1.979	1.991
O(5)	1.879	1.823	1.849
V_-	0.128	0.124	0.144
V_+	−0.244	−0.226	−0.218
T_c (K)	92.3	83.0	79.1

The error bar for V_- at one point was estimated from allowing the atomic structure to vary within one standard deviation of the best result obtained from neutron diffraction. The $x=0.1$ sample in Fig. 9 (open circle with the smallest T_c) which as mentioned is slightly above the solubility limit of the orthorhombic phase, displays an anomalously large V_-. This is consistent with some additional Ca in the 123 structure, beyond the maximum Th doping level.

The inset of Fig. 9 illustrates that V_- for Ca-Th doping also behaves differently than for Ca-Pr doping in 123 compounds. Although the errors are here somewhat larger, V_- clearly decreases with Ca-Pr doping, albeit more slowly than for charge doped systems.

One can also note from Tables II and III that V_- for the pure Y compound is larger than for Nd-123 by about 0.06, which can be almost entirely accounted for by the larger Cu2 valence. Such an increase in Cu2 valence with decreasing size of the Y-site ion has been observed previously for a series of RE-123 samples.[19]

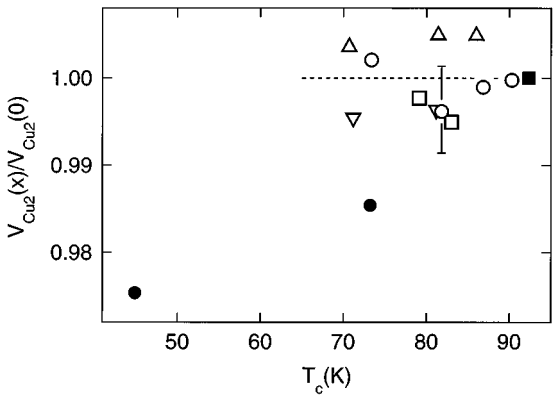

FIG. 8. Normalized Cu2 valence vs T_c for Ca_xTh_x doped Nd-123 (○) (present data), and Y-123 (□) (Ref. 2), Ca_xPr_x doped Nd-123 (△) (Ref. 6), and Y-123 (▽) (Ref. 16), and for Pr_x doped Y-123 (●) (Ref. 17). Calculations similar to the present ones were made from data of Ref. 17 for Pr doping. The solid square contains the measured T_c for all nondoped samples.

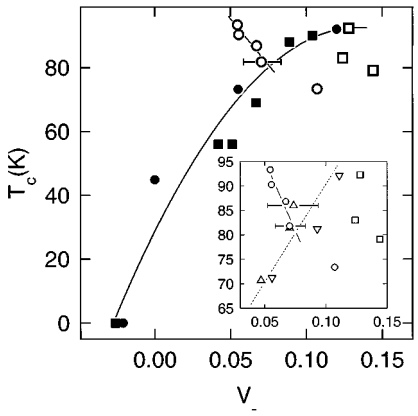

FIG. 9. T_c vs total hole doping in the plane (V_-) for Ca-Th doped Nd-123 (○) (present data) and Y-123 (□) (Ref. 2), Pr doped Y-123 (●) (Ref. 17), and oxygen doped Y-123 (■) (Ref. 18). The line is a fit of a straight line to the $Nd_{1-2x}Ca_xTh_xBa_2Cu_3O_{7-\delta}$ data up to $x=0.05$. The curve is a guide to the eye. Inset: Ca-Th doping (same symbols as in main panel) compared to Ca-Pr doping in Nd-123 (△) (Ref. 6) and Y-123 (▽) (Ref. 16). The bars illustrate estimated errors of (V_-). The lines are guides to the eye. The data suggest different mechanisms for the depression of T_c with Ca-Th and Ca-Pr doping.

IV. SUMMARY AND DISCUSSION

A. Main results for Ca-Th doped Nd-123

Sintered samples of $Nd_{1-2x}Ca_xTh_xBa_2Cu_3O_{7-\delta}$ have been studied by electrical resistance measurements and by x-ray and neutron diffraction. The solubility limit in the orthorhombic phase is slightly below $x=0.1$ as inferred from x-ray diffraction, and transport properties in the superconducting and normal states. The structural changes with doping were small, with a small decrease of the c-axis length and cell volume. The oxygen concentration was almost constant with increased oxygen disorder and decreased orthorhombicity. The Cu1-O4 distance remained almost constant with doping, while the Cu2-O4 bond length displayed a small increase.

The superconducting critical temperature, T_c, decreased linearly at the rate of $-dT_c/dx$ of about 230 K. To our knowledge this strong effect is the largest depression rate observed in a charge neutrally doped high-temperature superconductor. It is an interesting problem to understand why Ca-Th doping has this detrimental effect on superconductivity.

B. Differences and similarities between Ca-Th and Ca-Pr doping in 123

It is useful to summarize various properties of Ca-Th doped Nd-123 by comparing with Ca-Pr in the same host,[6] and with Ca-Th and Ca-Pr doping in Y-123.[2,16] The linear depression of T_c, the constant Cu2 valence, and the nearly constant oxygen level support a charge neutral doping in all four systems. Changes in structure and bond lengths as observed by neutron diffraction are small and sometimes of variable sign. The Cu1-O4 distance e.g., is within experimental uncertainty almost constant for Ca-Th doping, while it increases slightly for Ca-Pr in Y-123 and decreases for Ca-Pr in Nd-123. Therefore, it appears that there is no simple relation between T_c and this bond length.

An interesting common trend in a bond length change is the increase of the Cu2-O4 distance with doping in all four systems illustrated in Fig. 7. Presently available data do not allow for more detailed comparisons. It is interesting to note, however, that the smallest rate of increase of the Cu2-O4 bond length occurs for Ca-Pr doped Y-123,[20] which also has the smallest depression rate of T_c ($-dT_c/dx \approx 100$ K), while the stronger rate of increase of the Cu2-O4 bond length within the solubility limit in the two Nd-based systems and in the Y-Ca-Th system correspond to a depression rate about twice as large.

Closer inspection of the results show some differences between Ca-Th and Ca-Pr doping. When going from Ca-Th doped Y-123 to Nd-123, the depression rate increases by about 30%. For Ca-Pr doped compounds the corresponding increase of the depression rate is larger than a factor of 2, suggesting that the effect of the size of the Y-site ion on the depression rate is quite different for Ca-Th and Ca-Pr doping.

From the BVS results, V_+, measuring the tendency for holes on oxygen in the CuO_2 planes, increases with decreasing T_c for Ca-Th doped samples. This is in contrast to Ca-Pr doped systems,[6] where instead V_+ decreased with decreasing T_c, as expected for optimally doped ceramic samples.[12] Furthermore, it was found previously that the hole density in the planes, V_-, decreased with doping of Ca-Pr.[6] For Ca-Th doping in contrast V_- remains almost constant. These trends in BVS results indicate interesting differences between Ca-Pr and Ca-Th doping in 123 hosts (Fig. 9). Apparently significant charge transfers, albeit small, occur, which cannot be easily resolved from studies of bond lengths only, but are clearly seen in BVS calculations.

One must ask what causes the strong depression of T_c in these samples? Ca-Th doping in 123 compounds is charge neutral, as for Ca-Pr doping, magnetic interactions do not seem likely, which is one suggestion for the T_c depression with Ca-Pr doping, and in contrast to Ca-Pr doping no significant depletion of charge appears in the CuO_2 planes. Yet the depression of T_c is stronger for Ca-Th than for Ca-Pr doping.

It is interesting to observe that the increase of the resistivity at 275 K of Ca-Th doped Nd-123 for $0 \leqslant x \leqslant 0.05$, shown in Fig. 4, is much stronger than for the corresponding Ca-Pr doped samples,[6] and the decrease of the temperature coefficient of resistance over the same concentration range is also considerably stronger. Both these changes are in the direction expected for weakening metallic properties due to electronic disorder, and a comparison between Fig. 4 and Ref. 6 thus suggests that such disorder effects are stronger when substituting with Ca-Th than with Ca-Pr. This possibility would seem to merit further investigations.

ACKNOWLEDGMENTS

We would like to thank Håkan Rundlöf, Studsvik, for skilled assistance with the neutron-data collection. This work was supported by the Swedish Natural Science Research Council, and by the Swedish Superconductivity Consortium.

[1] M. Andersson, Z. Hegedüs, M. Nygren, and Ö. Rapp, Physica C **160**, 65 (1989).
[2] M. Andersson, Ö. Rapp, and R. Tellgren, Solid State Commun. **81**, 425 (1992).
[3] O. Hartmann, E. Karlsson, E. Lindström, R. Wäppling, P. Lundqvist, Z. Hegedüs, and Ö. Rapp, Physica C **235–240**, 1695 (1994).
[4] J. J. Neumeier, T. Björnholm, M. B. Maple, and I. Schuller, Phys. Rev. Lett. **63**, 2516 (1989).
[5] J. Fink, N. Nücker, H. Romberg, M. Alexander, M. B. Maple, J. J. Neumeier, and J. W. Allen, Phys. Rev. B **42**, 4823 (1990).
[6] P. Lundqvist, C. Tengroth, Ö. Rapp, R. Tellgren, and Z. Hegedüs, Physica C **269**, 231 (1996).
[7] M. Andersson, Ö. Rapp, T. L. Wen, Z. Hegedüs, and M. Nygren, Phys. Rev. B **48**, 7590 (1993).
[8] K. E. Johansson and P. E. Werner, J. Phys. E **13**, 1289 (1989).
[9] H. M. Rietveld, J. Appl. Crystallogr. **2**, 65 (1969).
[10] J. Rodriguez-Carvajal, e-mail: juan@bali.saclay.cea.fr.
[11] I. D. Brown and D. Altermatt, Acta Crystallogr. Sec. B **41**, 244 (1985).
[12] J. L. Tallon, Physica C **168**, 85 (1990).
[13] I. D. Brown, J. Solid State Chem. **82**, 122 (1989).
[14] Y. Ren, H. B. Tang, Q. W. Yan, P. L. Zhang, Y. L. Liu, C. G. Qui, T. S. Ning, and Z. Zhang, Phys. Rev. B **38**, 11 861 (1988).
[15] R. D. Shannon, Acta Crystallogr. Sec. A **32**, 751 (1976).
[16] M. Andersson, Ö. Rapp, and R. Tellgren, Physica C **205**, 105 (1993).
[17] J. J. Neumeier, T. Björnholm, M. B. Maple, J. J. Rhyne, and J. A. Gotaas, Physica C **166**, 191 (1990).
[18] R. J. Cava, A. W. Hewat, E. A. Hewat, B. Batlogg, M. Marezio, K. M. Rabe, J. J. Krajeweski, W. F. Peck, and L. W. Rupp, Physica C **165**, 419 (1990).
[19] S. Ramesh and M. S. Hedge, Physica C **230**, 135 (1994).
[20] There are only two data points for Ca-Pr doped Y-123 in Fig. 7. However, the result for $x=0.2$ from Ref. 16, still within the solubility limit for this alloy system, confirms this small increase of bond length.